MINISTRY OF EDUCATION AND TRAINING

VIETNAM NATIONAL CHEMICAL GROUP

VIETNAM INSTITUTE OF INDUSTRIAL CHEMISTRY

TRAN THI LIEN

SYNTHESIS AND CHARACTERISTIC OF CATALYST SYSTEMS BASED ON Pt/rGO AND Pd/rGO APPLIED IN ELECTRO-OXIDATION REACTION OF ALCOHOL C_1 AND C_2

Specialty: Theoretical Chemisty and Physical Chemistry Code: 9.44.01.19

SUMMARY OF DOCTORAL THESIS

Hanoi -2020

The thesis completed at:

Vietnam Institute of Industrial Chemistry

Scientific instructors:

1. **Prof.Ph.D. Vu Thi Thu Ha**
2. **Prof.Ph.D. Le Quoc Hung**

Reviewers:

1. **Assoc.Prof.Ph.D. Vu Thi Thu Ha**
2. **Ph.D. Nguyen Tran Hung**
3. **Assoc.Prof.Ph.D. Nguyen Thi Cam Ha**

LIST OF PUBLISHED SCIENTIFIC WORKS

1. Vũ Thị Thu Hà, Nguyễn Minh Đăng, Vũ Tuấn Anh, **Trần Thị Liên**, Nguyễn Quang Minh. *Nghiên cứu độ ổn định hoạt tính oxi hóa điện hóa methanol và ethanol của xúc tác Pt-AlOOH-SiO_2/rGO*; Tạp chí Xúc tác Hấp phụ, Tập 5, Số 4 (2016).
2. Thu Ha Thi Vu, Léa Vilcocq, **Lien Tran Thi**, Luis Cardenas, Thanh Thuy Thi Tran, Francisco J. Cadete Santos Aires, Bui Ngoc Quynh, Nadine Essayem. *Influence of platinum precusor on electrocatalytic activity of Pt/rGO catalyst for methanol oxidation.* Tạp chí Xúc tác và Hấp phụ, Tập 5, số 2, trang 128-134 (2016).
3. Vũ Thị Thu Hà, **Trần Thị Liên**, Nguyễn Minh Đăng, Nguyễn Quang Minh, Nguyễn Thị Thảo, Vũ Tuấn Anh. *Tổng hợp xúc tác PtMe/rGO (Me=Ni, Co, Al, Al-Si) có hoạt tính điện hóa cao trong phản ứng oxi hóa ethanol*. Tạp chí Khoa học và Công nghệ Việt Nam, T16, số 5, trang 12-16 (2017).
4. **Tran L. T**., Nguyen Q. M., Nguyen M. D., Thi Le H. N., Nguyen T. T., & Thi Vu T. H. *Preparation and electrocatalytic characteristics of the Pt-based anode catalysts for ethanol oxidation in acid and alkaline media.* International Journal of Hydrogen Energy. Volume 43, Issue 45, Pages 20563-20572 (2018).
5. **Tran LT**, Tran TTT, Le HNT, Nguyen QM, Nguyen MD, et al. *Green Synthesis of Reduced Graphene Oxide Nanosheets using Shikimic Acid for Supercapacitors*. J Chem Sci Eng, 2(1): 45-52 (2019).
6. Minh Dang Nguyen, **Lien Thi Tran**, Quang Minh Nguyen, Thao Thi Nguyen, and Thu Ha Thi Vu. *Enhancing Activity of Pd-Based/rGO Catalysts by Al-Si-Na Addition in Ethanol Electrooxidation in Alkaline Medium.* Journal of Chemistry, Vol. 2019, Article ID 6842849, 13 pages (2019).

A- INTRODUCTION

1. Rationale of the thesis

Due to the gradual exhaustion of fossil fuels and its adverse impact on the environment, the need of developing renewable and sustainable energy sources becomes increasingly essential. In this context, fuel cells in general and fuel cells using direct alcohol (DAFC) in particular have received special attention from scientists because of their excellent energy conversion efficiency and almost zero pollution producing.

Among the traditional catalysts applied for DAFC batteries, the bulk Pt catalyst have been extensively studied due to its high electrochemical oxidation activity of alcohols. However, high cost and easy catalytic poisoning by intermediate compounds generated during the oxidation of alcohol are barriers in the commercialization of this device. An effective way to enhance the stability of the catalyst, and to prevent the loss of Pt active phases, is to disperse them on a suitable support at the nanoscale. Graphene with outstanding physicochemical properties is currently one of the most potential candidates owning to its well-suited requirements such as: high specific surface area; strong pressure to metal nanoparticles to ensure their effective fixation capacity; high conductivity helping electronical transfer occur rapidly in various redox reactions; high chemical stability in the reaction medium to maintain a stable catalytic structure. By tentative studies, it is expected that graphene could bring more benefits to the electrochemical catalyst. On the other hand, for the purpose of reducing the cost of DAFC batteries, many Pt-M alloy catalysts carried on graphene have been studied, most of which are, typically, based on noble metals and transition metals such as Pd, Au. , Co, Ni, Ag, Fe, etc. In general, the modified catalysts often exhibit higher electrochemical activity than the single-metal catalyst Pt/graphene. In addition, the presence of the promotion phase has the effect of changing the electronic band structure, thereby reducing the adsorption energy of the intermediate compound CO_{ads} on the catalyst surface, leading to increasing possibility of poisoning and increasing activity endurance for Pt/graphene catalysts.

Staying in the trend of the world, studies of graphene and DAFC are also getting much attention from domestic scientists. Especially, since 2012, National Key Laboratory for Petrochemical and Refinery Technologies has studied the catalysts based on Pt/graphene applied to DAFC batteries and so far continues to pursue this new research direction. Within the framework of the research directions of National Key Laboratory for Petrochemical and Refinery Technologies, this thesis aims to find a new method to synthesize graphene supports, dispersing evenly the Pt particles at the nanoscale; to change and combine different components in the promotion phase to enhance the properties and durability of Pt/graphene catalyst activity. On this basis, the thesis will concentrate on modification of Pt/graphene-based catalyst with high electrochemical activity and minimizing the use of noble metals such as Pt, applied in the oxidation reactions of short chain alcohols (methanol, ethanol).

This is an open research direction with scientific and practical significance, and it is hoped that the results of the thesis will contribute to promoting the development of graphene and Pt/graphene-based catalysts for catalytic processes in general and manufacturing DAFC in particular.

2. Research objectives and contents

The thesis aims to study the process synthesis of Pt-based and Pd-based anode catalysts for DMFC and DEFC, contributing to significantly reduce amount of noble metals used in catalysts, resulting in lower manufacturing cost of fuel cells. To achieve this goal, the thesis focuses on the following main studies:

- Researching and exploring the use of shikimic acid - reducing agents which has plant source - in the synthesis of graphene (rGO), applied as a metal catalyst support in the electro-oxidation reaction of methanol and ethanol;
- Studying the process of synthesizing rGO-based catalysts by flexibly changing existing synthesis methods (wet-chemical method, co-reduction, hydrothermal, physically assisted

reduction method) depending on according to each promotion phase object;

- On the basis of the results of previous research, modify of Pt-based/rGO catalysts by common and cheaper metals such as (Al, Si, Co, Ni) is conducted to create nanocomposites Pt-M/rGO with high electrocatalytic performance and good antipoisoning ability in the oxidation reaction of methanol and ethanol;
- Investigating the electrochemical activity of Pt-M/rGO catalysts systematically in both acidic and base medium, thereby selecting effective and suitable catalysts applied as anode catalyst in DMFC and DEFC;
- Investigating and comparing electrochemical activity between Pd-based/rGO catalysts and Pt-M/rGO catalysts in ethanol oxidation reaction.

3. The scientific and practice meaning of the thesis

Contributing to the knowledge of graphene synthesis and catalysts based on noble metals (Pt, Pd) supported on graphene with high electroactivity, applied in direct alcohol fuel cells (DAFC) in general and DMFC, DEFC in particular.

The thesis meets practical needs of increasing the efficiency of electrochemical catalysts while minimizing the use of noble metal Pt, contributing to the development of renewable energy sources - fuel cells.

4. The new contributions of the thesis

- Systematically investigated Pt/rGO catalysts doped by compounds of different metals (M = Al, Si, Al-Si, Co, Ni, Co-Ni) in the ethanol oxidation reaction in acidic and base medium. Successfully synthesized PAS/rGO and PA/rGO catalysts with high electrochemical activity and stability in both acidic and base medium. In EOR, the electrocatalytic activity of PA/rGO is ~3.6 times higher (in acidic medium) and ~1.6 times (in base medium); the activity durability of PA/rGO is ~9 times higher (in acidic medium) and ~7 times (in base medium) than that of non-doped Pt/rGO catalysts;
- Successfully synthesized PdAS/rGO doped by Al-Si oxide

complex, giving high electrocatalytic activity (7822 mA mg_{Pd}^{-1}) in EOR in base medium. PdAS/rGO catalyst also exhibits activity durability by maintaining a current density of 104.4 mA mg_{Pd}^{-1} after 4000 s of durability test – 1.1 times higher than that of PA/rGO catalyst at the same conditions. The successful doping of Pt/rGO and Pd/graphene catalysts with common and cheap metals in general and Al, Si in particular has contributed to enhancing the efficiency of electrochemical catalysts and significantly reducing amount of noble metal used in catalysis, leading to decreased costs of DAFC;

- Systematically studying method of graphene preparation by reducing GO by reducing ethylene glycol and shikimic acid. Research results on plant-based reducing agents - shikimic acid - contribute to the diversification of reducing agents in graphene synthesis. On the other hand, this result opens the direction of synthesis without using toxic chemicals, of being environmentally friendly, suitable for the needs of graphene applied in the field of bio-medicine and other special purposes.

5. Layout of the thesis

The thesis consists of 140 pages, 16 tables, 54 figures divided into sections: Introduction (2 pages), Chapter 1 Overview (47 pages), Chapter 2 Experiment (20 pages), Chapter 3 Results and Discussion (49 pages), Conclusion (2 pages), New contributions (1 page); List of published works (1 page); References including 205 references (17 pages).

B – MAIN CONTENT

CHAPTER 1: OVERVIEW

This chapter presents an overview of structure, properties and methods of synthesizing graphene materials, and introduced direct ancohol fuel cells (DAFC) and the graphene-based electrocatalysts applied in DAFC in general and DMFC, DEFC in particular. The overview also presents the synthesis and catalytic modification methods based on graphene supports applied to fuel cells.

CHAPTER 2 : EXPERIMENT

2.1. Preparation of graphene

Graphene oxide (GO) was first synthesized by modified Hummer method. Graphene (rGO) was then prepared by reducing the GO in the presence of reducing agent ethylene glycol or shikimic acid.

2.2. Preparation of Pt-based catalyst supported on graphene

The Pt/rGO catalyst containing 40 wt% Pt (theoretically calculated) compared to rGO was prepared from GO, EG and H_2PtCl_6 by the reflux method.

2.3. Preparation of the Pt-based catalysts doped by Al or Al-Si supported on graphene

The PAS/rGO catalyst was synthesized from GO, TEOS, Al-isopropoxide, IPA, EG and H_2PtCl_6, having a mass ratio (theoretically calculated) corresponding to the total content of Al and Si of 7 wt% and Pt 40 wt% compared to rGO. The obtained catalysts containing the Al and Si compositions exist as pseudo-boehmite (AlOOH) and silica (SiO_2).

The PA/rGO catalyst was synthesized in a similar way as the PASG catalyst, however, in the absence of the Si precursor during synthesis. The PAG catalyst has compositions (theoretically calculated) corresponding to the content of Al of 20 wt% and Pt 20 wt% compared to rGO.

2.4. Preparation of the Pt-based catalyst doped by Si supported on graphene

The PS/rGO catalyst was synthesized by the solvothermal method, with a calculated Si and Pt content (theoretically calculated) of 5 wt% and Pt 40 wt%, compared to rGO.

2.5. Preparation of the Pt-based catalysts doped by Co or/and Ni supported on graphene

The catalyst containing 20 wt% Co or Ni and 5 wt% Pt (theoretically calculated) compared to rGO, denoted as PC/rGO and PN/rGO respectively, was synthesized by using $Co(CH_3COO)_2.4H_2O$ and $Ni(CH_3COO)_2.4H_2O$ precursors, respectively. Similarly, the PCN/rGO catalyst containing 30 wt% for each of Co and Ni, and 20 wt% Pt (theoretically calculated) compared to rGO was synthesized,

however, using both $Co(CH_3COO)_2.4H_2O$ and $Ni(CH_3COO)_2.4H_2O$ precursors at the same time.

2.6. Preparation of Pd-based catalyst supported on graphene

The catalysts with compositions: Pd/rGO, Pd-Al/rGO, Pd-Si/rGO and Pd-Al-Si/rGO denoted as Pd/rGO, PdA/rGO, PdS/rGO and PdAS/rGO. These catalysts was synthesized in a similar way to the catalysts containing Pt, respectively: Pt/rGO, PA/rGO, PS/rGO và PAS/rGO according to the procedures described above; only replace the precursor H_2PtCl_6 with the precursor $PdCl_2$. The mass ratio of the active phase compared to rGO (theoretically calculated) remained unchanged.

2.7. Physicochemical characterization

The synthesized catalysts are evaluated by the modern methods of TGA, XRD, SEM, TEM, Raman, ICP-OES and XPS.

2.8. Electrochemical characterization

- CV and CA measurements were carried out in NaOH 0.5 M + C_2H_5OH/CH_3OH 1 M or H_2SO_4 0.5 M + C_2H_5OH/CH_3OH 1 M aqueous solutions at a scan rate of 50 mV s^{-1}.
  - The CV tests were carried out in the potential range of -0.2 to 1.0 V in acid medium and from -0.8 to 0.5 V in base medium.
  - The CA curves for the catalysts were recorded in acid medium at a constant potential value of 0.7 V and in base medium at a constant potential value of -0.2 V (vs. SCE for 4000 s).
- In order to determine the reaction products, The reaction products were identified by using a high performance liquid chromatograph (HPLC) equipped with a UV detector and a refractive index detector. The analysis conditions and schematic for trapping the outlet products before HPLC analysis were described in Fig. 2.1. However, in base medium, the first flask was replaced with a flask containing H_2SO_4. After electrolysis experiments, the volatile compounds were transported by nitrogen flow.

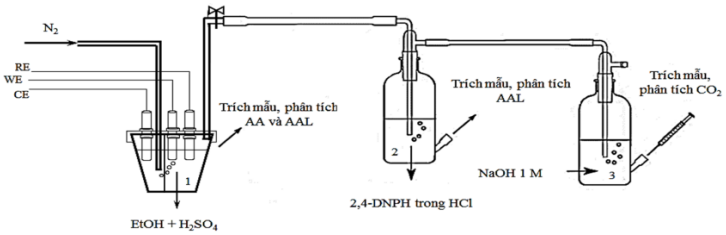

Fig. 2.1. Experimental set-up to trap the reaction products at the outlet of the DEFC before HPLC analysis

CHAPTER 3. RESULTS AND DISCUSSION

3.1. Synthesis and characteristic properties of graphene

TEM images (Fig.3.1) shows that GO has the structure of micrometer-sized spread sheets with many wrinkles, while TEM images of rGO exhibits that after reduction, graphene sheets kept its own super thin and almost transparent sheet structure.

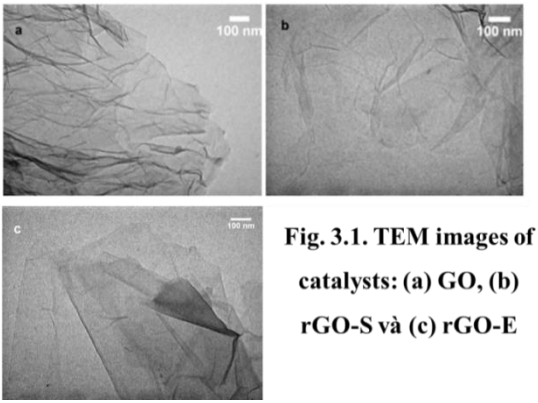

Fig. 3.1. TEM images of catalysts: (a) GO, (b) rGO-S và (c) rGO-E

After reduction, a series of XRD pattern (Fig. 3.2) of rGO-E and rGO-S demonstrates the disappearance of the peak located at 10.6°, while a broad diffraction peak attributed to the (002) carbon peak of rGO appears at ca. 24°÷26° (2θ), implying that GO was successfully reduced to rGO by using EG or acid shikimic.

Raman spectra (Fig. 3.3) shows that the D band of graphene oxide exhibits a much lower intensity for the G band, so the I_D/I_G ratio

below 1. This is the identication of a decrease in the average size of the sp^2 domain. On the contrary, the I_D/I_G ratio increases after the reduction process, which indicates that there are more defects in the graphene composites, caused by reducing agents, thus reducing the size of the graphitic domains.

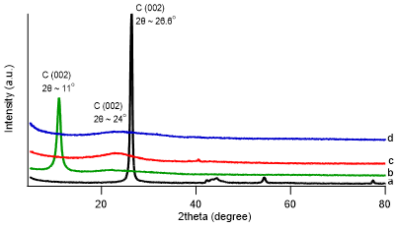

Fig. 3.2: XRD patterns of a-graphite, b-GO, c- rGO-E and d- rGO-S

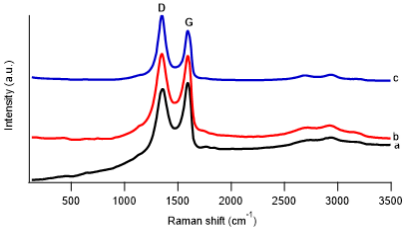

Fig. 3.3: Raman spectra of a- GO, b-rGO-E and c- rGO-S

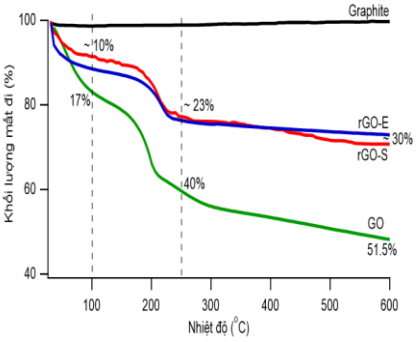

Fig. 3.4: TGA plots of graphite, GO, rGO-E and rGO-S

TGA plots (Fig 3.4) demonstrate that the total weight loss after the heating to 600 ºC was ~30% for both rGO-E and rGO-S (29.3% for rGO-S and 27.6% for rGO-E), less than that of GO, which indicated that there was a significant decrease in the amount of functional groups on material surface after reduction, or to put it in other way, GO was successfully reduced to rGO by EG and shikimic.

Due to the high cost of shikimic acid refining process, it is not suitable with the objective of the catalytic synthesis process that the thesis aims to. Meanwhile, the characteristic results show that both graphene rGO-S and rGO-E are completely similar in physical-chemical propeties and microstructure, and can be applied as catalyst

support. Therefore, the EG reducing agent was chosen for the subsequent experiments because of availability in the laboratory.

3.2. Catalyst Pt/graphene (Pt/rGO)

3.2.1. Characterization of Pt/rGO catalyst

TEM image (Fig. 3.6) of Pt/rGO exhibits that Pt particles are small (2 ÷ 10 nm) but mainly distributed in the size range of 2 ÷ 5 nm, scattered on graphene surface. The presence of Pt particles is also evidenced by the XRD patternt (Fig. 3.5) with the appearance of typical reflection peaks at 2θ values of about 39.5°, 46.8° and 68° could be attributed to the characteristic (111), (200) and (220) planes of face-centered-cubic (fcc) crystalline structure Pt. After reduction, the typical (002) reflection peak of GO at 2θ ~11° is completely disappeared and a board peak between 2θ ~24° – 26° is observed on the spectra of Pt/rGO indicating GO is effectively reduced.

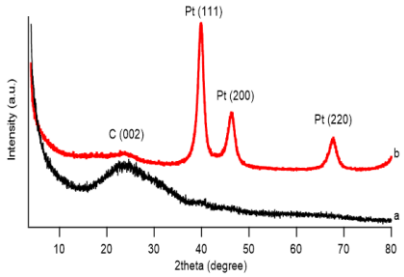

Fig. 3.5. XRD patterns of catalysts (a) rGO and (b) Pt/rGO

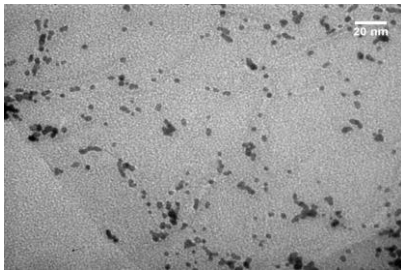

Fig. 3.6. TEM image of Pt/rGO catalyst

3.2.2. Electrochemical activity of Pt/rGO catalyst for MOR and EOR

Observations of figures 3.7, 3.8, 3.9 and 3.10 show that, Pt/rGO catalysts exhibit the same trend of reaction in both MOR and EOR. Indeed, the electroactivity in base medium many times higher than that of acid medium, expressed as I_F and ECSA current density values are shown in Table 3.1.

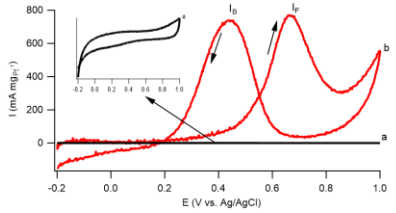

Fig. 3.7. CV curves of catalysts in CH_3OH 1 M + H_2SO_4 0.5 M solution at scan rate 50 mV s^{-1}: (a) rGO and (b) Pt/rGO

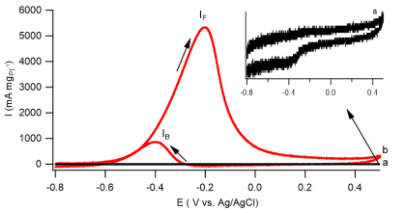

Fig. 3.8. CV curves of catalysts in CH_3OH 1 M + NaOH 0.5 M solution at scan rate 50 mV s^{-1}: (a) rGO and (b) Pt/rGO

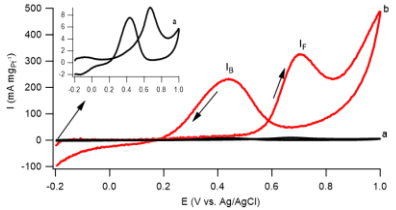

Fig. 3.9. CV curves of catalysts in C_2H_5OH 1 M + H_2SO_4 0.5 M solution at scan rate 50 mV s^{-1}: (a) rGO and (b) Pt/rGO

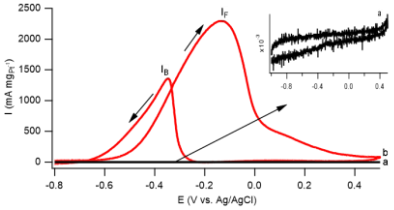

Fig. 3.10. CV curves of catalysts in C_2H_5OH 1 M + NaOH 0.5 M solution at scan rate 50 mV s^{-1}: (a) rGO and (b) Pt/rGO

Table 3.1. Electroactivity of Pt/rGO catalyst for MOR and EOR in two reaction media

Peak current density I_F (mA mg_{Pt}^{-1})			
H_2SO_4 0,5 M + MeOH 1 M	*NaOH 0.5 M + MeOH 1 M*	*H_2SO_4 0.5 M + EtOH 1 M*	*NaOH 0.5 M + EtOH 1 M*
765	**5348**	**328**	**2293**
Electrochemical acitive surface area ECSA (m^2 g_{Pt}^{-1})			
H_2SO_4 0,5 M		*NaOH 00.5 M*	
34.88		**103.64**	

In addition, it can be seen that the prepared Pt/rGO catalyst has many times more electroactivity when compared with the commercial catalyst 40% Pt/C under the same reaction conditions.

3.3. Modify Pt/rGO catalyst (Pt-M/rGO, M= Al, Si, Al-Si, Co, Ni, Co-Ni)

3.3.1. Characterization of Pt-M/rGO catalysts

After reduction, a series of XRD pattern of different catalysts shown in Fig. 3.11b-h demonstrates the disappearance of the peak located at 10.6°, while a broad diffraction peak attributed to the (002) carbon peak of rGO appears at ca. 24.4° (2θ), implying that GO was successfully reduced to rGO. In the case of PAS/rGO and PS/rGO catalysts, because of the resonance effect between the diffraction peak at 24-26° ascribed to the signal of amorphous silica and the diffraction peak (002) of rGO, the intensity of the peak at 2θ is higher than that of other catalysts. Similar to our previous works, no typical diffraction peaks of aluminum-based compounds appeared in Fig. 3.11c and 3.11e, suggesting that doped Al was formed as either amorphous or nanocrystalline particles in the PAG and PASG catalysts.

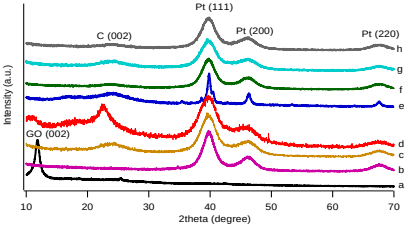

Fig. 3.11. XRD patterns of: (a) GO, (b) Pt/rGO,(c) PAS/ rGO, (d) PS/ rGO, (e) PA/ rGO, (f) PCN/ rGO, (g) PC/ rGO and (h) PN/ rGO

As shown in Fig. 3.11b, for the Pt/rGO catalyst, the typical reflection peaks at 2θ values of about 39.5°, 46.8° and 68° could be attributed to the characteristic (111), (200) and (220) planes of face-centered-cubic (fcc) crystalline structure Pt (JCPDS No. 04-0802 Card). Compared with Pt/rGO, it is easy to see on the XRD patterns of all Pt-M/rGO samples (Figure 3.11c - h), these peaks are slightly shifted to a higher 2θ angle, showing the presence of the doped phase (M) changed the crystal structure. Indeed, the XRD pattern of samples containing Co and /or Ni (Fig. 3.11f –h) shows diffraction peaks at angles 2θ ≈ 40,2o, 47,1 and 68,5, respectively. for the (111), (200) and (220) planes of the alloys PtCo and PtNi. On the other hand, no characteristic peaks of Co, Ni or its oxides/hydroxides can

be observed from Fig. 3.11f -h, and this suggest that the Co, Ni nanoparticles exist in the form of alloys PtCo, PtNi.

As shown in this Fig. 3.12a, the sheet structure in a large area of the rGO. It can be easily observed that PG, PASG and PSG catalysts have similar nanostructure and size, differing only in the dispersion. The Pt nanoparticles of the PG catalyst have an average particle size of about 3 nm, with a relatively sparse distribution (Fig. 3.12b). The PASG and PSG catalysts exhibit a dense but uniform dispersion of metallic nanoparticles, with the mean particle size of 2.5 ÷ 2.8 nm (Fig. 3.12c-d). For the PAG catalysts (Fig. 3.12e), Pt nanoparticles size is also about 2.5 nm in average, distributed evenly, but with less density than the two PASG and PSG catalysts. It might result from the Pt content (theoretically calculated) of the PAG catalyst being the only half of the two PASG and PSG catalysts.

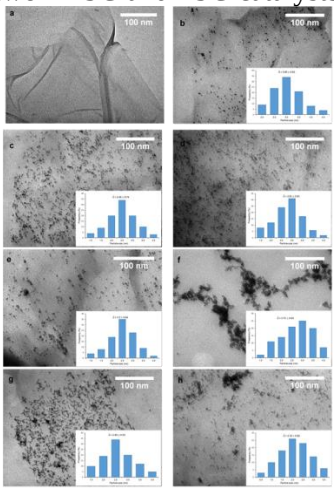

Fig. 3.12. TEM images of different catalysts: (a) rGO, (b) Pt/rGO, (c) PAS/rGO, (d) PS/rGO, (e) PA/rGO, (f) PCN/rGO, (g) PC/rGO và (h) PN/rGO

For the PCNG catalyst (Fig. 3.12f), Pt, Co, Ni content (theoretically calculated) was 20%, 30%, 30%, respectively. The metallic nanoparticles do not disperse uniformly but agglomerate into "cords", which overlap with each other to form a "dendrite" structure. For the PCG sample (Fig. 3.12g), Pt, Co content (theoretically calculated) was 5%, 20%; the dispersion of the metal nanoparticles improved significantly. As observed in Fig. 2g, besides

the monoparticles, there are quite a number of nanoclusters, which are shaped "zigzag", formed by the aggregation of 3-4 monoparticles. In the case of the PNG catalyst, the appearance of metallic monoparticles, with an average size of about 2.1 nm, was discretely distributed alongside the clusters of the size of tens to hundreds nm (Fig. 3.12h).

The Pt content and the compositions of active phase are determined by the ICP-OES method. It can be seen that the Pt content found in most catalysts is about 50% of the theoretical mass, although the Pt content varies between 5÷40%.

Compared with Pt/rGO catalyst, the XPS survey spectrum of the PAG catalyst exhibits not only the characteristic peaks of C 1s, O1s and Pt 4f, but also two peaks of Al 2s and Al 2p located at ca. 120 and 75 eV, respectively. It can be easily seen that the binding energies value of Pt (0) and Pt (II) species of Pt/rGO catalyst are slightly lower than that of PA/rGO catalyst, meaning that interaction ability of Pt species with supports is stronger in the presence of Al.

In summary, the results of chemical and physical characteristics proved that the presence of modified phase, specially the Pt-AlOOH structure, which improves the dispersion of the promotion phase, and reduces the agglomeration of the Pt nanoparticles, enhancing the contact between Pt active sites and reactant molecules.

3.3.2. Electrochemical activity of Pt-M/rGO catalysts

3.3.2.1. Electrochemical activity of Pt-M/rGO catalysts for EOR

Table 3.2. Summary of ECSA values of different Pt-based/graphene electrocatalysts in two media

Catalyst	ECSA in acid medium ($m^2\ g^{-1}_{Pt}$)	ECSA in base medium ($m^2\ g^{-1}_{Pt}$)
Pt/rGO	34.88	103.64
PS/rGO	40.77	112.82
PAS/rGO	66.09	165.13
PA/rGO	**121.20**	**188.48**
PCN/rGO	60.64	94.67
PC/rGO	79.73	126.53
PN/rGO	94.77	159.35

It can be clearly seen that, in both reaction media, Pt-based binary and ternary catalysts gave higher ECSA than monometallic Pt catalyst (Table 3.2), and furthermore, all catalysts gave higher ECSA in base medium than in acid medium. The fact that more metal nanoparticles dispersed on the graphene sheet surface would cause more uniform dispersion of these sheets by preventing aggregation between them, which led to producing many more accesible pt active sites. As a result, the larger ECSA values of multimetallic catalysts are obtained.

Table 3.3. The CV results of different Pt-based/graphene electrocatalysts in two media (25ºC)

Catalyst	Peak current density I_F (mA mg_{Pt}^{-1})	
	H_2SO_4 0.5 M + Ethanol 1 M	NaOH 0.5 M + Ethanol 1 M
Pt/rGO	328	2293
PS/rGO	391	2299
PAS/rGO	872	3518
PA/rGO	**1194**	**3691**
PCN/rGO	878	2257
PC/rGO	959	2550
PN/rGO	1054	2966

As it can be seen, in both acid and base media, Pt-based catalysts undoped by other metals (Pt/rGO) have significantly lower the oxidative electrochemistry than that of catalysts doped (Fig. 3.13, 3.14 and Table 3.3). It is remarkable to note that the PA/rGO catalyst has the highest activity out of the evaluated catalysts in both reaction media. It is higher than the reported works for catalysts based on modified Pt/rGO reaching 3480 mA mg^{-1}_{Pt} and especially, is many times higher than the electroactivity of the commercial Pt/C in acid medium – 3.44 mA mg^{-1}_{Pt} and base medium - 36 mA mg^{-1}_{Pt}, respectively.

The improvement of the deposition of metal nanoparticles on the surface of rGO can be explained by the presence of Al. Indeed, by comparing the percentage of $\%Pt_d/\%Pt_i$ ($\%Pt_d$ is the content Pt deposited on graphene calculated according to ICP-OES, $\%Pt_i$ is the

theoretically calculated Pt initial content) of the PG and PAG catalysts, it is evident that PAG catalyst showed higher percentage of $\%Pt_d/\%Pt_i$ (80.5 %) than PG catalyst (73.5 %). Moreover, the presence of Al also improved the dispersion of the Pt nanoparticles on the support surface, hence, increasing the electro-active sites, which is in reasonable agreement with the TEM and XPS results.

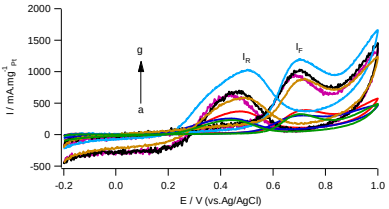

Fig. 3.13. CV curves of catalysts in H_2SO_4 0.5 M + C_2H_5OH 1 M solution, at scan rate 50 mV s^{-1}: (a) Pt/rGO, (b) PS/rGO, (c) PAS/rGO, (d) PCN/rGO, (e) PC/rGO, (f) PN/rGO and (g) PA/rGO

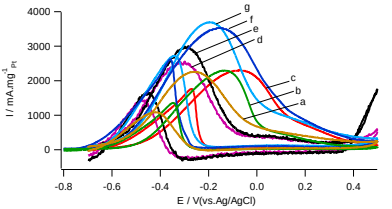

Fig. 3.14. CV curves of catalysts in NaOH 0.5 M + C_2H_5OH 1 M solution at scan rate 50 mV s^{-1}: (a) PCN/rGO, (b) Pr/rGO, (c) PS/rGO, (d) PC/rGO, (e) PN/rGO, (f) PAS/rGO and (g) PA/rGO

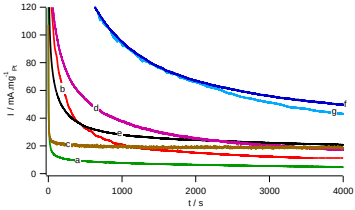

Fig. 3.15. CA curves of catalysts in H_2SO_4 0.5 M + C_2H_5OH 1 M solution at potential of 0,7 V: (a) Pt/rGO, (b) PS/rGO, (c) PCN/rGO, (d) PC/rGO, (e) PN/rGO, (f) PAS/rGO and (g) PA/rGO

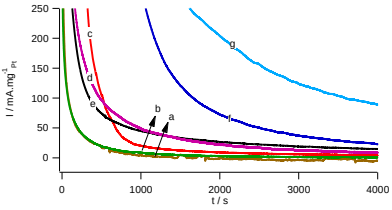

Fig. 3.16. CA curves of catalysts in NaOH 0.5 M + C_2H_5OH 1 M solution at potential of -0,2 V: (a) PCN/rGO, (b) Pt/rGO, (c) PS/rGO, (d) PC/rGO,(e) PN/rGO, (f) PAS/rGO and (g) PA/rGO

Among the surveyed catalysts, both PAG and PASG catalysts exhibited better electrochemical stability compared to the other catalysts in both media. In an acid medium (Fig. 3.15), the PASG catalyst exhibits moderate activity (only higher than that of the PG catalyst), yet good stability. After 4000 s, the retained current density of the PASG catalyst is 49.8 mA mg^{-1}_{Pt}, which is equivalent to the value obtained for the PAG catalyst (43.0 mA mg^{-1}_{Pt}) and greatly higher than the value obtained for PG (4.8 mA mg^{-1}_{Pt}) catalyst. It is caused by the fact that the presence of SiO_2 - an unique oxide that forms hydroxyl species even in the acidic pH. These groups ($–OH_{ad}$) will reacts with CO_{ads} on the Pt surface via Langmuir-Hinshelwood mechanism. In the base medium, after 4000 s, the remaining current density of the PAG catalyst was 89.1 mA mg^{-1}_{Pt} (higher than ~7 times compared with Pt/rGO catalyst) and that of the PASG catalyst was 22.8 mA mg^{-1}_{Pt} (Fig. 3.16).

On the other hand, the CA measurement results of the two catalysts PA/rGO and PAS/rGO in two different electrolyte (H_2SO_4 and NaOH) showed a more rapid decrease in current over time in base medium, even though the current started out higher in magnitude. This has been observed previously in the literature and can be attributed to the anion ((bi(sulfate)) adsorption phenomena in acid medium.

The HPLC analysis results shows that the reaction products analyzed consist of acetic acid (AA, in the form of acetate in base solutions), acetaldehyde (AAL) và CO_2 (in the form of carbonate in base solutions) with different composition ratios depending on the catalysts and the reaction media. In acid medium, the main product obtained is AAL for all catalysts and remarkable difference between AAL and AA is observed. A small amount of CO_2 (< 3%) is also detected. In base medium, chemical yield of AAL and AA show no difference. Notably, CO_2 content, which is a final product of EOR, increased more significantly than in acid medium, indicating that the CO_2 formation could be favoured and more facile than in base medium. Indeed, for both media, the presence of promoters phase helped binary and ternary catalysts consume more ethanol than Pt-only catalysts. Most strikingly, the amount of ethanol consumption

for the PAG catalyst is 2.3 times and 1.5 times higher than PG in acid and base media, respectively.

3.3.2.2. Electrochemical activity of PA/rGO and PAS/rGO catalysts for MOR

The electrocatalytic activity of PA/rGO for MOR shows mass activity (2924 mA mg_{Pt}^{-1} in acid medium and 9682 mA mg_{Pt}^{-1} in base medium) is ~2.5 and ~2.6 times higher than that of PAS/rGO catalyst for EOR, respectively. In the acid medium, although the shape of the CV curves of the catalysts in MOR and EOR is the same but the onset and anode peak potentials in the EOR have more positive shifts compared to the MOR (E_{onset} from 0.20 V to 0.22 V, E_{If} from 0.665 V to 0.770 V). This is explained by the fact that the presence of C-C bonds in EOR requires higher energy to break than in MOR. Similar to EOR in base medium, in MOR, the catalysts of PA/rGO and PAS/rGO (Fig. 3.18) also showed many times higher electrochemical activity than acid medium (Fig. 3.17).

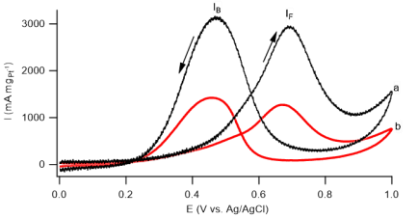

Fig. 3.17. CV curves of catalysts in CH_3OH 1 M + H_2SO_4 0.5 M solution at scan rate of 50 mV s^{-1}: (a) PA/rGO and (b) PAS/rGO

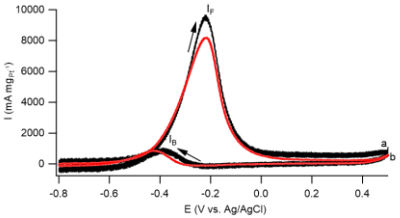

Fig. 3.18. CV curves of catalysts in CH_3OH 1 M + NaOH 0.5 M solution at scan rate of 50 mV s^{-1}: (a) PA/rGO and (b) PAS/rGO

However, in the EOR, the I_F/I_B ratio is not too large (< 2) but in MOR, the I_F/I_B ratio greatly increases. This phenomenon is explained by the adsorption of (bi)carbonate in the NaOH medium. The (bi)carbonate formed can prevent a complete surface oxide (PtO) layer from forming. As the potential is swept cathodically, the oxide is reduced, but the (bi)carbonate remains adsorbed onto the Pt surface. With a lower number of surface sites available for MeOH

adsorption as compared to the anodic sweep, a decrease in current (I_B) is observed in MOR.

3.3.3. Examination of the durability of PAS/rGO and PA/rGO catalysts for MOR and EOR

3.3.3.1. Examination of the durability of PAS/rGO catalyst for MOR and EOR

The results of durability test in MOR (Fig. 3.19 and 3.20) showed that in base medium, after only 300 cycles, the peak current density lost of 56%, in contrast, after 1200 cycles in acid medium electroactivity of PAS/rGO remained very high, only reduced by 19%. This finding is in agreement with the CA results mentioned above.

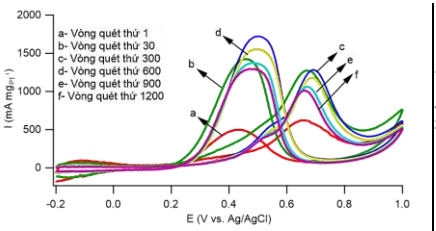

Fig. 3.19. CV curves of PAS/rGO catalyst for 1200 cycles in CH_3OH 1 M + H_2SO_4 0.5 M at scan rate of 50 mV s^{-1}

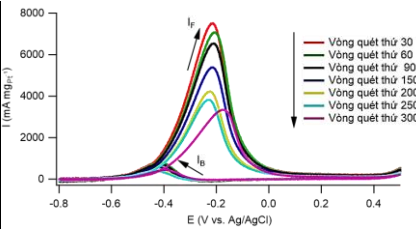

Fig. 3.20. CV curves of PAS/rGO catalyst for 300 cycles in CH_3OH 1 M + NaOH 0,5 M at scan rate of 50 mV s^{-1}

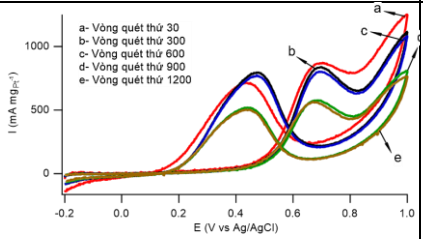

Fig. 3.21. CV curves of PAS/rGO catalyst for 1200 cycles in C_2H_5OH 1 M + H_2SO_4 0.5 M at scan rate of 50 mV s^{-1}

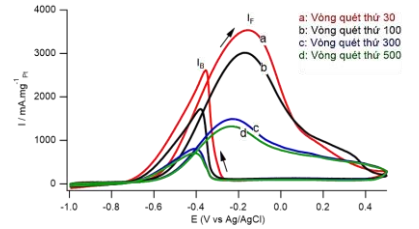

Fig. 3.22. CV curves of PAS/rGO catalyst for 500 cycles in C_2H_5OH 1M +NaOH 0.5 M at scan rate of 50 mV s^{-1}

Similar to the case of methanol, the PAS/rGO catalyst has high durability and stability in the oxidation of ethanol in acid medium,

corresponding to a decrease of current density of 35% after 1200 cycles of scanning; meanwhile, in base medium, the electroactivity decreased by 62% of the initial value after only 500 cycles (Fig. 3.21 and 3.22).

TEM images (Fig. 3.23) of the PAS/rGO catalyst after durability test showed that after 500 cycles in base medium, the metal particles on the surface of rGO had agglomerated and morphologically changed into large size clusters with discrete distribution. Meanwhile, after 1200 scans in acid, the metal particles on the rGO surface agglomerated into nanorod structures (from 70÷200 nm long and ~25 nm horizontally), distributing into separate clusters on the rGO support.

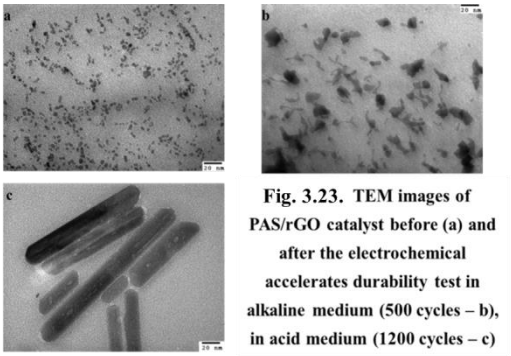

Fig. 3.23. TEM images of PAS/rGO catalyst before (a) and after the electrochemical accelerates durability test in alkaline medium (500 cycles – b), in acid medium (1200 cycles – c)

3.3.3.2. Examination of the durability of PA/rGO catalysts for MOR and EOR

The reaction trend was still the same as PAS/rGO, for MOR (Fig 3.24-25) in the base medium, the decrease in activity occurred faster and deeper than in the acid medium. This phenomenon is explained by the fact that when (bi)sulfate adsorbs to the Pt surface diminishing the overall current, it also prevents the formation of CO_{ads}. Therefore, (bi)sulfate inhibits MeOH adsorption, resulting in a lower initial current for the MeOH in H_2SO_4, but it also inhibits CO adsorption, resulting in a slower current decay in acid medium.The results of durability test in EOR (Fig 3.26-27) showed that after 300 cycles, in acid medium, the peak current density of the modified electrode

shows a slight change, loss of 15% but decreases at a relatively fast rate (49%) in base medium. Therefore, a durability test was extended to 1200 cycles in acid medium and the current density of PAG nanocatalyst was reduced by 55% of its initial.

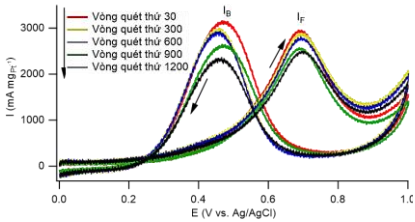

Fig. 3.24. CV curves of PA/rGO catalyst for 1200 cycles in CH_3OH 1 M + H_2SO_4 0.5 M at scan rate of 50 mV s^{-1}

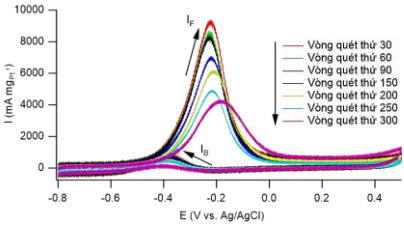

Fig. 3.25. CV curves of PA/rGO catalyst for 300 cycles in CH_3OH 1 M + NaOH 0.5 M at scan rate of 50 mV s^{-1}

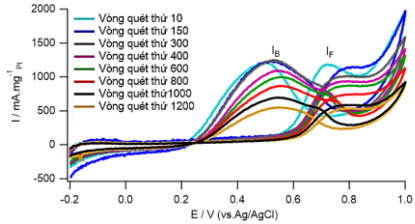

Fig. 3.26. CV curves of PAS/rGO catalyst for 1200 cycles in C_2H_5OH 1 M + H_2SO_4 0.5 M at scan rate of 50 mV s^{-1}

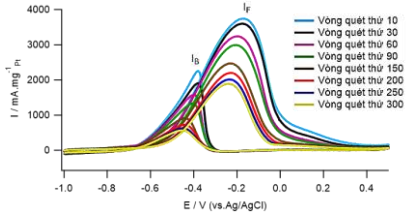

Fig. 3.27. CV curves of PAS/rGO catalyst for 300 cycles in C_2H_5OH 1 M +NaOH 0.5 M at scan rate of 50 mV s^{-1}

The change in morphology and microstructure before and after the durability test of PAG catalyst estimated by TEM is shown in Fig. 3.28. In base medium, after 300 scanning cycles, severe agglomeration with the formation of Pt nanocluster of approximately 100 nm (Fig. 3.28b) is observed, which results in a notable reduction in catalytic activity after 300 scanning cycles. In acid solution, after 1200 scanning cycles, the morphology and size of the Pt nanoparticles in PAG catalyst show a small change, from 2.5 to 3.8

nm and the density of the Pt nanoparticles on the surface decreases, while that of the particles at the edges of the graphene sheet increases (Fig. 3.28c-d). This might result from the appearance of chemical defects of post-reduction graphene. The durability test proved that the PAG nanocatalyst had the high durability and stability, reasonably attributed to the special Pt-AlOOH structure, which improves the dispersion of the promotion phase, and reduces the agglomeration of the Pt nanoparticles, enhancing the contact between Pt active sites and reactant molecules.

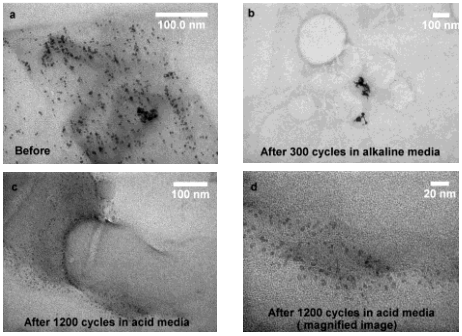

Fig. 3.28. TEM images of PAG catalyst before (a) and after the electrochemical accelerated durability test in base medium (300 cycles – b), in acid medium (1200 cycles – c, d), at a scan rate of 50 mV s^{-1}

3.4. Study on preparation, modification and characterization of Pd-based/graphene application in ethanol oxidation reaction

TEM image of Pd/rGO (Fig. 3.29) showed that Pd nanoparticles were uniform and homogenous dispersion on support surface with the mean particle size of 2÷5 nm. In addition, they tend to agglomerate with high density at the edges of graphene sheet or along the wrinkles on surface. TEM images of Pd-M/G catalysts exhibited a more sparse distribution of particles, metallic nanoparticles scattered on the support, no agglomeration and the size of particles was quite similar (~2,3 ÷ 2,8 nm). The microstructure of rGO sheet in multimetallic catalysts almost did not overlap,

particularly, on the surface of the PdA/rGO catalyst,"cracks" appearred.

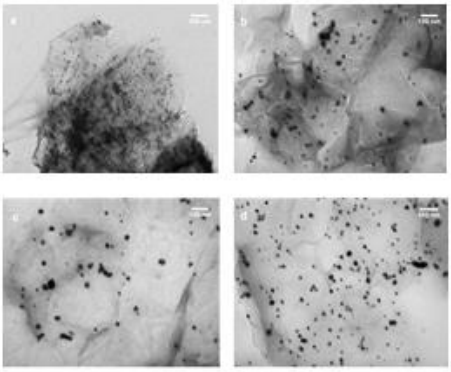

Fig. 3.35. TEM images of the different catalysts: a- Pd/rGO, b- PdA/rGO, c- PdS/rGO and d- PdAS/rGO

The investigated electroacitvity results are presented in Table 3.4 and Fig. 3.30. Among the surveyed catalysts, PdAS/rGO gave the highest current density value of 7822 mA mg_{Pd}^{-1}. Moreover, after 4000 s of durability test, PdAS/rGO catalyst also maintained better current density to 104.4 mA mg_{Pd}^{-1}. In general, the trend of reaction with PAS/rGO catalyst can be attributed to the improvement of activity and durability of PdAS/rGO hybrid catalyst due to the presence of AlOOH-SiO_2 hybrid complex. This combination not only improves the dispersion of Pd nanoparticles better, decreases the cover by intermediate products, thereby increasing the ability to contact between Pt active sites and reactant ethanol molecules, but also highlights the ability to provide $–OH_{ads}$ groups that help minimize the impact of CO_{ads} on catalysis.

Table 3.4. The electroactivity of different Pd-based/graphene catalysts in NaOH 0.5 M + C_2H_5OH 1 M solution

Catalyst	**I_F** / mA mg_{Pd}^{-1}	**I_B** / mA mg_{Pd}^{-1}	**I_F/I_B**
Pd/rGO	5369	3915	1.37
PdA/rGO	5374	3799	1.41
PdS/rGO	5574	4010	1.39
PdAS/rGO	**7822**	**6111**	**1.28**

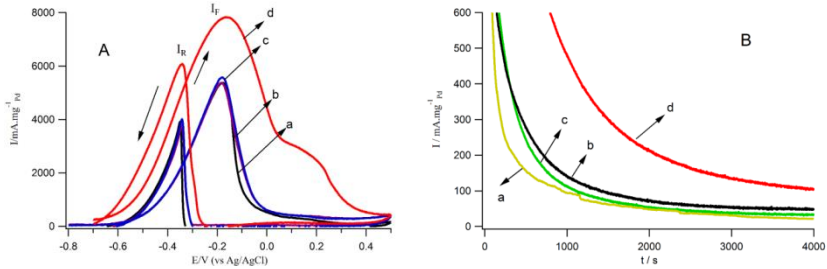

Fig. 3.30. CV curves (A) and CA curves (B) of catalysts in NaOH 0.5 M + C_2H_5OH 1 M solution at scan rate of 50 mV s^{-1}:(a) Pd/rGO, (b) PdA/rGO, (c) PdS/rGO và (d) PdAS/rGO

There are several similarities for both catalysts involving in the EOR. That includes the functionality as the base catalysts, the parameters affected the performance and the co-catalysts used. Because of that researchers can refer to Pt while developing for Pd in the aspect of performance and vice versa. It is not surprising since both catalysts belong in the same group and predictably, have similar characteristics and reactions.

CONCLUSION

1. Systematically studyed method of graphene preparation by reducing GO by reducing ethylene glycol and shikimic acid. The obtained results show that both graphene rGO-S and rGO-E are completely similar in physical-chemical propeties and microstructure, both graphene products can be applied as catalyst support. Research results on plant-based reducing agents - shikimic acid - contribute to the diversification of reducing agents in graphene synthesis. On the other hand, this result opens the direction of synthesis without using toxic chemicals, of being environmentally friendly, suitable for the needs of graphene applied in the field of bio-medicine and other special purposes.
2. Systematically investigated Pt/rGO catalysts doped by compounds of different metals (M = Al, Si, Al-Si, Co, Ni, Co-Ni) in the ethanol oxidation reaction in acidic and base medium. The obtained results indicated that in both media, the PA/rGO and PAS/rGO catalysts exhibits highest electroactivity and stability, notably:

- The Pt-based/rGO catalyst doped by Al (existing as pseudo-boehmit AlOOH) shows highest mass activity, corresponding to 1194 mA mg_{Pt}^{-1} (in acid medium) and 3691 mA mg_{Pt}^{-1} (in base medium). On the other hand, the activity durability of PA/rGO is ~9 times higher (in acidic medium) and ~7 times (in base medium) than that of non-doped Pt/rGO catalysts. The modified catalysts by compounds of Al or Al-Si complex not only increase the dispersion of the promotion phase, but also decrease the agglomeration of the Pt nanoparticles, thereby enhancing the contact between Pt active sites and reactant molecules, leading to a significant improvement in electrocatalytic activity and durability ;
- The results of durability test of PA/rGO catalyst showed that in base medium, the decrease of electroactivity occurred faster and deeper than in the acid medium. Indeed, after 1200 cycles in acid medium, the current density reduced by 55% and 49% (only after 300 cycles in base medium) of its initial value. The change in morphology and microstructure of Pt nanoparticles before and after the durability test of PA/rGO catalyst was estimated by TEM.

3. Successfully studied on Pt/rGO catalysts doped by Al and Al-Si combination, in the methanol oxidation reaction in acid and base medium.

- The obtained results indicated that in both reaction media, the PA/rGO catalyst exhibits higher electrocatalytic activity than that of PAS/rGO catalyst ;
- The electrocatalytic activity of PA/rGO for MOR shows mass activity (2924 mA mg_{Pt}^{-1} in acid medium and 9682 mA mg_{Pt}^{-1} in base medium) is ~2.5 and ~2.6 times higher than that of PAS/rGO catalyst for EOR, respectively.

4. Successfully synthesized PdAS/rGO doped by different metals: Al, Si, Al-Si oxide complex and identified the modified catalyst based on AlOOH-SiO_2 (PdAS/rGO) giving high electrocatalytic activity (7822 mA mg_{Pd}^{-1}) in EOR in base medium. PdAS/rGO catalyst also exhibits activity durability by maintaining a current density of 104.4 mA mg_{Pd}^{-1} after 4000 s of durability test – 1,1 times higher than that of PA/rGO catalyst at the same conditions.